ISSN 1726-5479

SENSORS & TRANSDUCERS

vol. 95
8/08

Sensors and Transducers Applications

International Frequency Sensor Association Publishing

IFSA

Sensors & Transducers

Volume 95
Issue 8
August 2008

www.sensorsportal.com

ISSN 1726-5479

Editor-in-Chief: professor Sergey Y. Yurish, phone: +34 696067716, fax: +34 93 4011989, e-mail: editor@sensorsportal.com

Sensors & Transducers Journal (ISSN 1726-5479) is a peer review international journal published monthly online by International Frequency Sensor Association (IFSA). Available in electronic and CD-ROM.

Sensors & Transducers Journal

Contents

Volume 95
Issue 8
August 2008

www.sensorsportal.com

ISSN 1726-5479

Research Articles

Authors are encouraged to submit article in MS Word (doc) and Acrobat (pdf) formats by e-mail: editor@sensorsportal.com
Please visit journal's webpage with preparation instructions: http://www.sensorsportal.com/HTML/DIGEST/Submition.htm

Sensors & Transducers Journal, Vol. 95, Issue 8, August 2008, pp. 26-39

Sensors & Transducers

ISSN 1726-5479

http://www.sensorsportal.com

Acoustic Wave Parameter Extraction with Application to Delay Line Modelling Using Finite Element Analysis

[1]Ajay Tikka, [1] Said Al-Sarawi and [2] Derek Abbott
[1]The Centre for High Performance Integrated Technologies and Systems (CHiPTec)
[2]Centre for Biomedical Engineering,
The University of Adelaide, SA 5005, Australia
E-mail: ajay.tikka@adelaide.edu.au

Received: 3 June 2008 /Accepted: 15 August 2008 /Published: 25 August 2008

Abstract: In this paper we propose a practical approach to develop a SAW parameter extraction technique and simulation method, contrary to the frequently used FEM/BEM numerical simulation technique. The new approach allows for accurate SAW device modelling through a versatile finite element method to automatically include the second order effects in the device by considering the complete set of partial differential equations. The eigenmodes and the harmonic admittance of a periodic structure obtained from the FEM simulations are used to extract the COM/P-matrix parameters based on a fitting technique that is already published in the literature. Comparison between the extracted parameters, using this technique, with currently published parameters for the same device specification was carried out and showed good agreement. As an example, a two dimensional delay line with 10 finger pairs per IDT was modelled using this approach, to outline the mechanical and electrical response of the device for variable acoustic modes and substrate thicknesses. *Copyright © 2008 IFSA.*

Keywords: Finite element analysis (FEA), Surface acoustic wave (SAW) devices, Bulk acoustic wave (BAW), Leaky surface acoustic wave (LSAW), Interdigital transducer (IDT), Coupling of modes analysis (COM), P-matrix model, Periodic boundary conditions (PBC)

1. Introduction

SAW devices have expanded into a multitude of products and applications in fields as diverse as microelectromechanical systems (MEMS), telecommunications, chemical sensing, and biotechnology [1, 2]. Precise characterization of SAW propagation parameters based on the device geometry and material characteristics is crucial for designing a SAW device. This is commonly performed by manufacturing a test structure, and then extracting the needed parameters through measurements. Such approach is both time consuming and expensive as each device optimization would require fabricating a test structure. On the other hand, precise numerical methods, mostly BEM/FEM analysis methods have been developed to optimize the design process [3, 4, 5]. In FEM/BEM models, the finite elements are used to account for the electrode shapes and the substrate is modelled as boundary elements. This is carried out by replacing the differential equations in the piezoelectric substrate by an integral equation at the boundary using Green's functions. Even though this results in a reduced computational time, the effects of mechanical perturbation, piezoelectric perturbation and energy storage caused by non-radiating bulk waves are not taken into consideration [6].

Considering the dramatic increase in computer performance, available at lower costs, switching from FEM/BEM analysis to finite element modelling (FEM) appears to be a logical choice, where the device is modelled by considering all the partial differential equations. In this paper FEM is used to model a periodic SAW structure to obtain the eigenmodes and harmonic admittance. However, it is important to keep using approximate analytical models like COM or P-matrix models in parallel, both to understand the basic physical behaviour and to validate the results obtained from finite element modelling. Therefore, apart from experimental validation, the extracted parameters of the periodic structure in FEM are in turn substituted in the analytical model to obtain the admittance response of a SAW component with longer length.

The FEM modelling of SAW devices was previously limited to either periodic structures or simple structures with few IDT electrodes [7, 8, 9]. With the availability of software packages with large node handling capability and an increase in computing performance and memory capacity, using direct FEM for numerical simulation of delay line with 10 finger pairs per IDT is feasible. In this paper the response of a delay line for different acoustic modes are analyzed through harmonic analysis. In addition to that, the effect of the piezoelectric substrate thickness on the output signal strength for Bulk and Leaky SAW (LSAW) modes are also discussed.

In Section 2, we discuss briefly the COM analysis and P-matrix model and highlight the parameters needed in this modelling approach. After the description of the periodic structure, we present the simulation results in Section 3, using modal and harmonic analysis. Then, in Section 4, we discuss how the needed parameters are extracted and compared to the experimental results in the literature. Finally, in Section 5, we present a 2-dimensional, 5 finger pairs per IDT delay line design. The admittance, output voltage response graphs and contour plots of displacement in the frequency domain are presented to illustrate the effect of all the acoustic modes on the delay line performance for two different piezoelectric substrate thicknesses.

2. COM and P-matrix Models

2.1. COM Model

Various numerical approximation and simulation techniques are available for the modelling and analysis of SAW devices. Coupling-of-modes (COM) is an accurate modelling approach where the excitation, propagation and scattering of surface acoustic waves are considered. The COM analysis is based on the Bragg condition, which states that the coupling between the incident and the reflected wave is strong if the period of the grating, p, is equal or close to half of the wavelength, λ, i.e $\lambda = 2p$. These waves form a stopband by interfering constructively and destructively at two discrete frequencies, where the propagation into the medium is minimum. As the incident wave and a reflecting wave have significant amplitudes compared to other harmonics only these waves may be considered in a stopband, resulting in a coupling of modes approximation.

In Fig. 1 *K(x)* and *L(x)* represent the counter propagating modes in the positive and negative *x* direction of the structure and *I(x)* the current caused by the induced charges in the electrodes when the transducer is driven by a Voltage *V*.

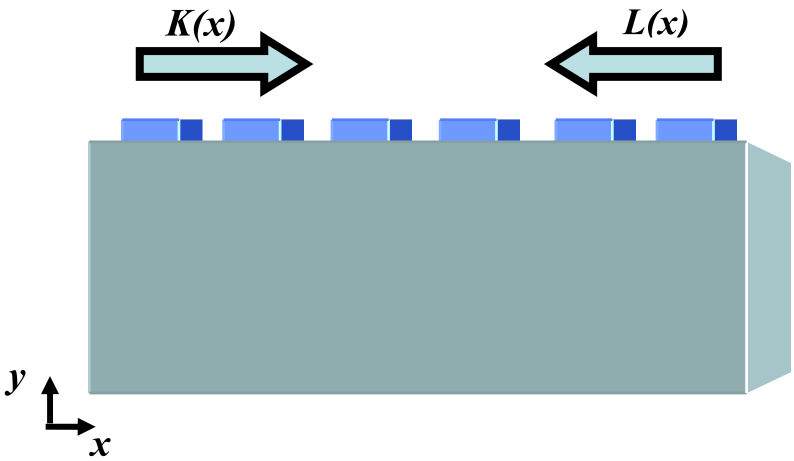

Fig. 1. SAW transducer with counter propagating modes.

Then the first order differential equations derived from the COM model are [10, 11]:

$$\frac{dK(x)}{dx} = -j\delta K(x) + j\kappa L(x) + j\alpha V, \tag{1}$$

$$\frac{dL(x)}{dx} = -j\kappa^* K(x) + j\delta L(x) + j\alpha^* V, \tag{2}$$

$$\frac{dI(x)}{dx} = -2j\alpha^* K(x) - 2j\alpha L(x) + j\omega CV. \tag{3}$$

where the independent parameters κ, α, v, γ and C are reflectivity due to perturbations, transduction coefficient, SAW velocity, attenuation, and capacitance per unit length, respectively. The asterisk denotes the complex conjugate.

In the above equations j is the imaginary term and δ is the detuning parameter given by

$$\delta = \frac{2\pi(f - f_0)}{v}$$

The centre frequency f_0 is given by $f_0 = V/2p$, where p is the period of the metal grating.

2.2. P-matrix Model

In some applications, the use of individual electrodes with varying properties is needed. Modelling such devices using COM model is ineffective. In such structures P-matrix model is an efficient modelling technique where the linear COM equations for each component are expressed as the elements of a matrix called P-matrix. The total response of the device can be determined by the cascading the P-matrices of all the individual components. These matrix elements and cascading techniques are explained in detail in [10, 12].

One of the important elements of the P-matrix is the admittance P_A, which depicts the electrical behaviour of a uniform bidirectional structure (IDT or a reflector) by relating the current I in the structure to the voltage V and given by [10].

$$P_A = P_A^M + P_A^E . \tag{4}$$

Here, P_A^M is the homogeneous component of the admittance which is determined by the eigenmodes,

$$P_A^M = -\frac{4\alpha^2(\delta+\kappa)}{n^3} \times \frac{(\delta+\kappa)(1-\cos(nL)) - jn\sin(nL)}{n\cos(nL) + j\delta\sin(nL)}, \tag{5}$$

where L is the length of the device and n is the slowly varying wavenumber of the eigenmode. While, P_A^E is the particular solution component of the admittance caused by the excited field, and given by

$$P_A^E = -j\left(\frac{4\alpha^2}{\delta-\kappa}L - \omega LC\right). \tag{6}$$

The P_A^E component dominates the admittance for long structures. This component of admittance is analyzed in the next section by substituting the extracted parameters from FEM simulations in Eqn. (6) for a specific device length.

3. Finite Element Modeling (FEM)

Field theory is the most appropriate theory for the design of SAW devices as it involves the resolution of all the partial differential equations for a given excitation. The Finite element model (FEM) is the most appropriate numerical representation of field theory where the piezoelectric behaviour of the SAW devices can be discretized and numerically solved [13]. As the standing waves are spatially periodic in SAW and BAW devices with the same grating shape and substrate, simulating a periodic substructure of the device to reduce the complexity and size of the numerical model might suffice. With the use of Periodic Boundary Conditions (PBC's) each mode that can be excited within the periodic structure can be modelled. As the periodic structure is part of the parent structure, the displacement and electric potential at both the left and right periodic boundaries are made equal. Due to large electrode apertures and predominantly lateral propagation of the surface acoustic waves, a plain strain condition is assumed to reduce the model to a 2D model [14]. In the following subsection we will discuss the simulation results.

3.1. Simulation Results

The simulations were carried out using ANSYS FEM package. For this purpose we consider a periodic structure, as shown in Fig. 2, having a 128º YX-cut $LiNbO_3$ piezoelectric substrate of length 1λ (λ = 4 μm), two Aluminium electrodes with a metallization ratio *MR* of 0.4, and an electrode thickness (h/λ) of *3%*. The material properties of the 12λ thick substrate were obtained from Ref. [15]. The PBC's are applied to the geometry as explained before and the results of the modal analysis and the harmonic analysis are presented in the following subsections.

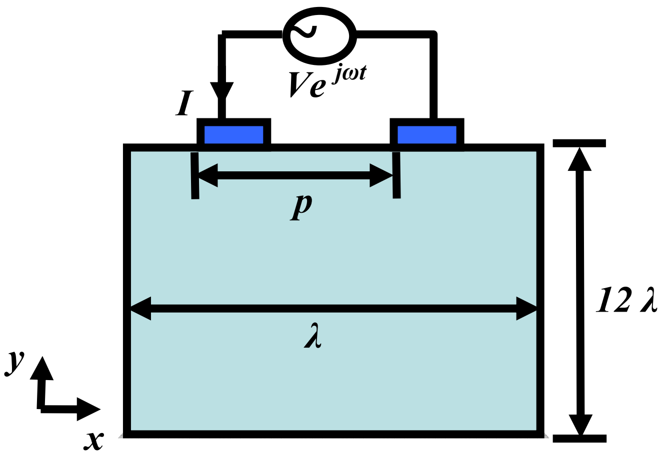

Fig. 2. Periodic structure.

3.1.1. Modal Analysis

The homogeneous solution of the differential equations involved in the FEM can be calculated using modal analysis to observe the eigenmodes propagating in the structure. The electrodes are shorted for this case and no external drive voltage is applied. By studying the mode shapes of the periodic structures the surface acoustic modes can be identified due to the confinement of the displacement at the top surface.

Two SAW modes were observed at frequencies of 907.4 MHz and 915.3 MHz for the periodic structure as shown in the Figs. 3(a) and 3(b). The differences in the deformation of the IDT's in both the modes can be used to identify the symmetric (f_{M-}) and anti-symmetric mode frequencies (f_{M+}) as explained in [14,16]. The IDT of the anti-symmetric SAW mode vibrates symmetrically about its centreline. The anti-symmetric SAW mode has a slightly higher frequency than the symmetric SAW mode as that type of vibration requires more strain energy. So from the SAW modal deformation in the Figs. 3(a) and 3(b), f_{M-} is 907.4 MHz and f_{M+} is 915.32 MHz.

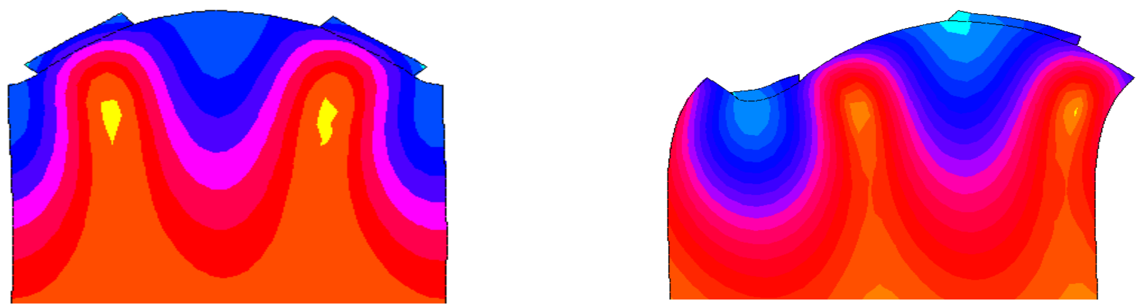

(a) (b)

Fig. 3. SAW modes (a) Symmetric SAW mode (f_{M-}) at 907.4 MHz
(b) Anti-symmetric SAW mode (f_{M+}) at 915.3 MHz.

3.1.2. Harmonic Analysis

The particular solution corresponding to the excited field of the differential equations can be obtained by using harmonic analysis. A drive voltage is applied across the electrodes and a steady state response is examined around the stopband edge frequencies, obtained from the modal analysis. All the nodes of the electrodes are coupled to keep the electric potential on the nodes constant. The displacement contour of the periodic structure is shown in the Fig. 4 when driven by a 2 V_{pp} voltage at a frequency of f_{M+}. It can be observed that the displacement is confined to the top surface of the structure with a maximum value of 0.644 nm close to the electrodes.

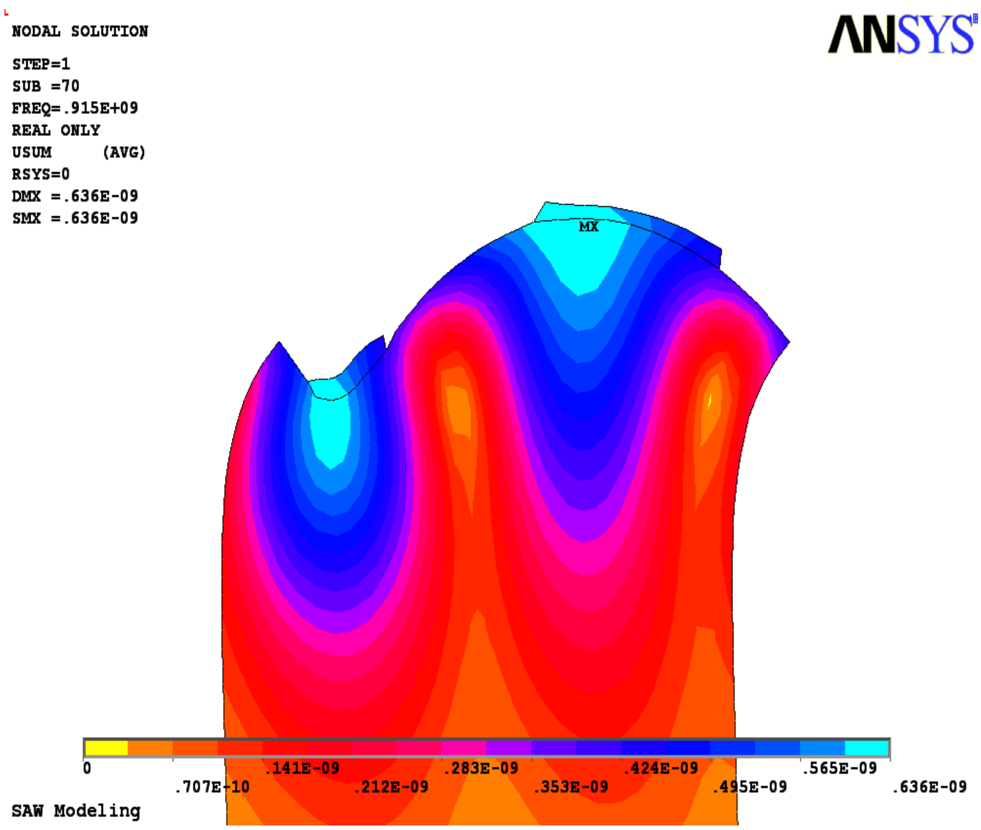

Fig. 4. Displacement Contour.

The harmonic admittance which characterizes the electrical behaviour of the SAW device can be determined from the complete charge distribution of the electrodes. If q is the complex charge of the electrode then the admittance Y is given by [8],

$$Y = j\frac{q\ \omega}{V}, \tag{7}$$

where ω is the angular frequency.

The admittance magnitude curve obtained from the FEM is depicted in the Fig. 5. It can be observed that the resonant peaks in the admittance curve coincide exactly with the stopband edge frequencies obtained from the modal analysis.

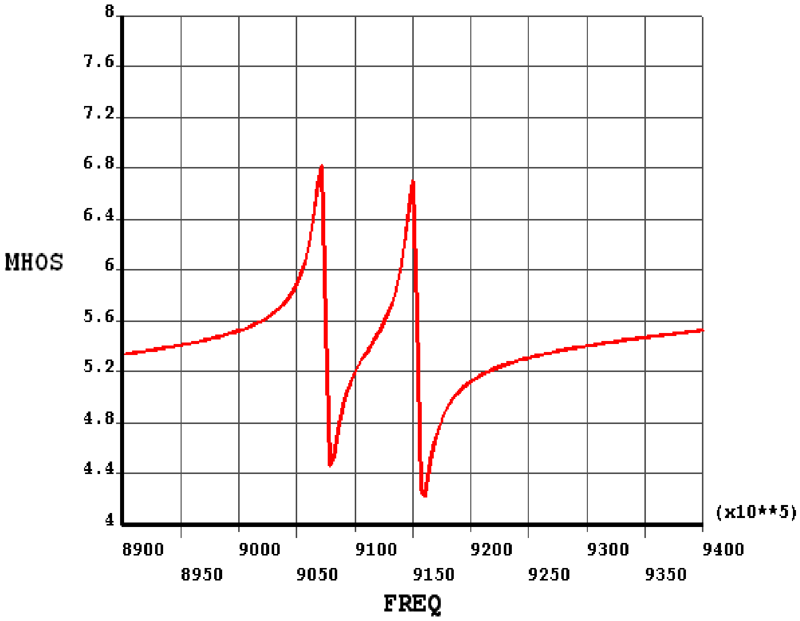

Fig. 5. FEM Admittance magnitude curve.

4. Parameter Extraction

The parameters in the COM equations (Eqn.(1) - (3)) are influenced by the material properties of the structures, crystal cut, shape of the electrodes, metallization ratio and aperture. To maintain a scale-invariant constants these parameters can be normalized to the periodicity and aperture *A* of the structure, as shown in Table 1. By computing the projection of FEM analysis onto the set of the field distributions predicted by the coupled-mode theory, we can derive the parameters corresponding to COM equations [6].

Table 1. Normalized COM Parameters [5].

Parameter	Symbol
Velocity	ν
Reflectivity	$\kappa_p = \kappa\,\lambda_0$
Transduction coefficient	$\alpha_p = \alpha\,\lambda_0$
Normalized transduction	$\alpha_n = \alpha_p / \sqrt{\frac{A}{\lambda_0}}$
Attenuation	$\gamma_p = \gamma\,\lambda_0$
Capacitance	$C_p = C\,\lambda_0$
Normalized Capacitance	$C_n = C_p/A$

The obtained short grated stopband edge frequencies (f_{M+} & f_{M-}) from the modal analysis can be substituted in Eqn. (8) and (9) to extract the velocity and reflectivity parameters for one period of the structure [10]. The sign of the reflectivity κ_p determines the location of the symmetric and anti-symmetric SAW modes.

$$v = p(f_{M-} + f_{M+}) \tag{8}$$

$$\kappa_p = \pi \frac{f_{M+} - f_{M-}}{f_{M+} + f_{M-}}. \quad (9)$$

All the other COM parameters can be determined from the characteristics of the curve, which is a direct representation of the electrical admittance of the experimental structure. A curve fitting technique is used to extract the parameters from the FEA computed admittance curve. This technique was employed earlier to determine the parameters of Green's function model [5]. The equations corresponding to this technique are presented below.

The P_A^E component in Eqn. (6) dominates the admittance for the infinitely long structures considered here. So the admittance for a periodic structure can be expressed as

$$Y = -j \frac{4\alpha^2 \lambda_0}{\delta + \kappa} L + j\omega C_p. \quad (10)$$

Let Y_r and Y_i denote the real and imaginary parts of the admittance in Fig. 6, respectively. The resonant frequency f_R, which is frequency at the peak of the real admittance $Y_{r\max}$ is given by

$$f_R = f_0 (1 - \frac{\kappa_p}{2\pi}). \quad (11)$$

and the peak of the real admittance part is

$$Y_{r\max} \equiv Y_R(f_R) = \frac{4\alpha_p^2}{\gamma_p}. \quad (12)$$

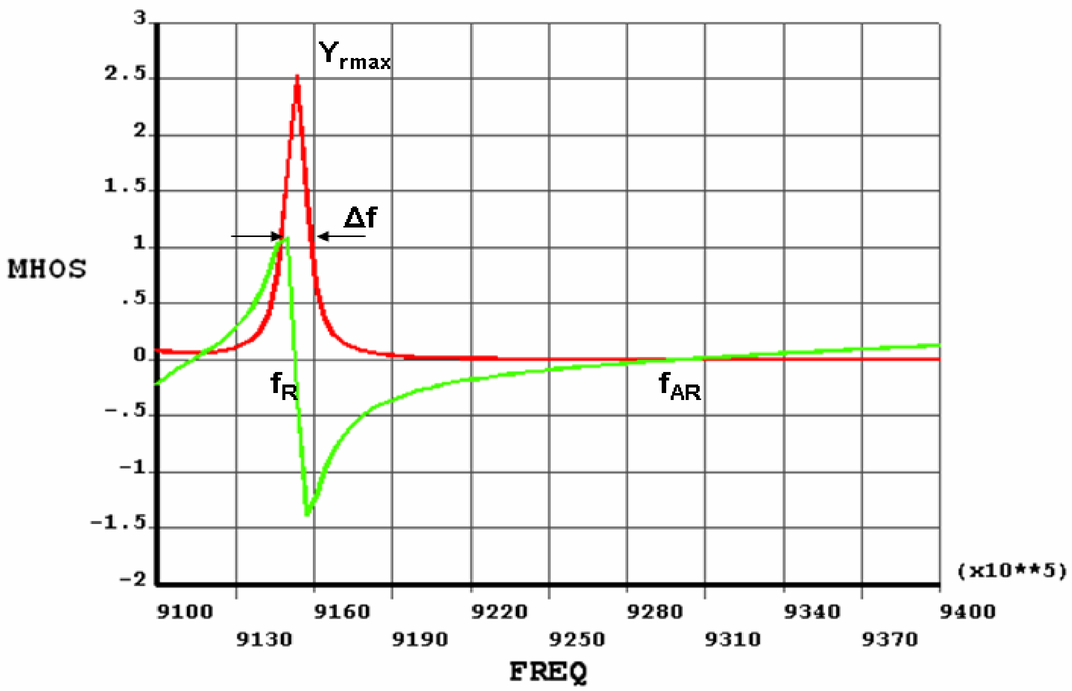

Fig. 6. FEM admittance curve with real and imaginary parts at f_{M+} mode frequency.

If Δf is the width of the real admittance peak at $Y_R = Y_{r\max}/2$ then

$$\Delta f = \frac{f_0 \gamma_p}{\pi} \tag{13}$$

All the information contained in the curve is described by the quantities in the above equations, from where the transduction coefficient α_p and the attenuation γ_p can be obtained.

The real and imaginary parts of the admittance can be expressed as:

$$Y_r(f) = \frac{Y_{r\max}}{4Q^2(f/f_R - 1)^2 + 1}, \tag{14}$$

and

$$Y_i(f) = -Y_{r\max}\frac{2Q(f/f_R - 1)}{4Q^2(f/f_R - 1)^2 + 1} + 2\pi f C_p. \tag{15}$$

As the imaginary part of the admittance crosses zero at the antiresonance frequency f_{AR} then Eq. (18) can be equated to zero at that frequency to find C_p

$$C_p = \frac{Y_{r\max}}{2\pi f_{AR}} \times \frac{2Q(f_{AR}/f_R - 1)}{4Q^2(f_{AR}/f_R - 1)^2 + 1},$$

where $Q = f_R/\Delta f$ is the quality factor.

All the COM parameters can be extracted by applying the Eqns. (10) - (16) to the observed quantities in the admittance curve of Fig. 6. The extracted parameters for SAW on 128º Y-cut X-propagating $LiNbO_3$ with rectangular aluminium for a metallization ratio (*MR*) of *0.4* and electrode thickness (*h*) of *3%* are presented in the Table 2 and compared with those in the literature [10] for the same device specifications. The velocity and the coupling constant are close to the corresponding values, which were reported in [10] and which were obtained using FEM/BEM analysis. The differences in the values of velocity can be attributed to mass loading effect and small SAW propagation in to the substrate. As there is no attenuation on the free surface in numerical simulations a small attenuation was introduced externally, which does not effect other parameters. The parameters α_n and C_n could not be compared with the one's in the literature because of the differences in the aperture length.

Table 2. COM Parameters for 128º YX-cut $LiNbO_3$ with MR of 0.4 and h of 3%.

Parameter	Current Work	[10]	Units
ν	3828	3885	m/s
κ_p	-0.024	-0.026	
α_n	41.5×10^{-5}		$\Omega^{-1/2}$
C_n	115.6×10^{-5}		pF/µm

The extracted parameters are substituted in Eqn. (9) for a structure length of *150λ* to get the COM/P-matrix admittance curve as shown in Fig. 7. The location of the resonant peak at centre frequency is in excellent agreement with the FEM simulations.

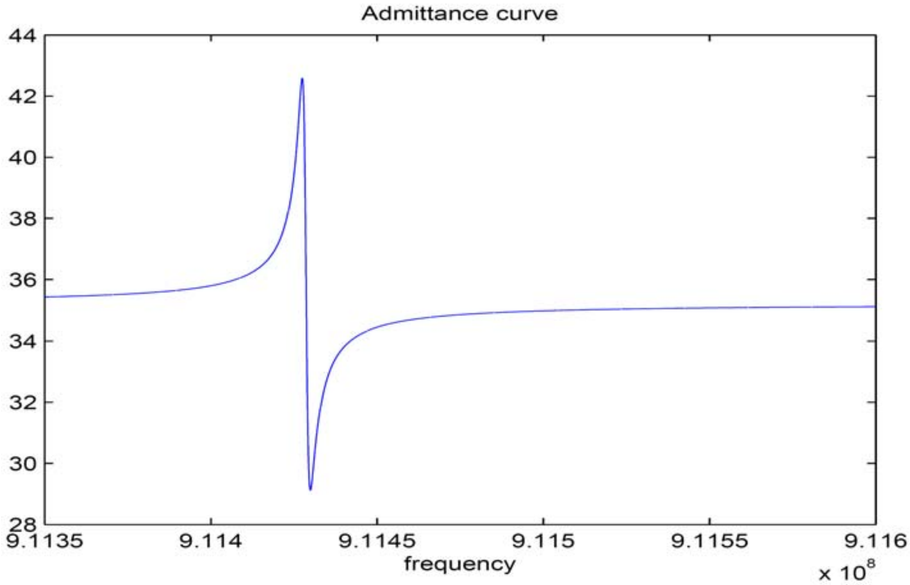

Fig. 7. Admittance curve from P-matrix using the extracted parameters.

5. Delay Line Optimization

Bulk and Leaky SAW mode characterization using FEM have been addressed considerably in the past using periodic structures [13, 17]. However, quantitative understanding of the effect these modes have on the correlator gain and the electromechanical coupling of a complete acoustic device remained to be a challenging problem in FEM. This is mainly due to huge constraint such modelling techniques placed on the available computational resources. With the rapid improvements made on the computational front recently it has become a possibility to model a complete delay line by neglecting features that contribute diminutively to the final output. Here we present an analysis of the effects various acoustic modes have on performance of a delay line and the way in which the response of the device can be optimized using the same direct finite element model developed for the characterization of surface acoustic waves and extraction of Coupling-Of-Modes (COM) parameters. In this paper the response of the delay line for different acoustic modes will be analyzed by performing a frequency sweep. In addition to that, the effect the piezoelectric substrate thickness would have on the output signal strength for bulk and Leaky SAW (LSAW) modes will also be presented.

5.1. Delay Line Modelling

A simple form of 2-dimensional 128° Y-cut X-propagating lithium niobate delay line comprising of two uniform input and output IDT's, as shown in the Fig. 8, is modelled in FEM. Both the input and the output transducers, having 20 electrodes each, were defined with a *MR* of 0.4, and an electrode thickness (h/λ) of *3%.* The separation between the input and the output transducer is taken to be 2λ (λ = 40 μm). The depth of the structure was chosen to be 10λ. Periodic boundary conditions were applied to allow minimal acoustic reflection at the finite-element model boundaries. The input IDT was driven by an alternating voltage of ±1V (2V peak to peak) to obtain the frequency response of the delay line. The harmonic analysis was carried out for a wide frequency range. Depending on the excitation frequency, various acoustic modes like the surface acoustic waves or bulk acoustic waves (BAWs) were excited. The admittance, output voltage response graphs and contour plots of displacement in the frequency domain are presented to illustrate the effect of bulk and leaky-SAW modes on the delay line performance for two different piezoelectric substrate thicknesses.

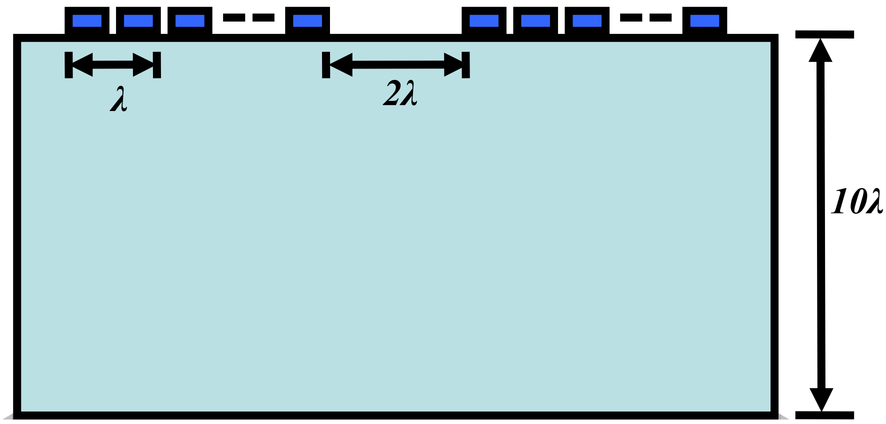

Fig. 8. Delay Line structure with 5 finger pairs per IDT.

The complex admittance of the device was computed based on the accumulated charge in the electrodes, as can be seen from the Fig. 9. The two admittance peaks to the left of the admittance curve, at frequencies of 90.6 MHz and 91.4 MHz, are the one's corresponding to the symmetric and anti-symmetric surface acoustic wave modes. The other admittance peaks correspond to bulk and leaky SAW modes can be verified with the help of contour plots. The displacement contours for SAW and LSAW modes are presented in the Figs. 11 & 12 respectively. From the LSAW mode displacement contour it can be clearly observed that the particle displacement is not just confined to the top surface as there are bulk wave components propagating through out the thickness of the substrate asserting the propagation characteristics of a LSAW mode.

Fig. 10 shows the output voltage response of the delay line for different acoustic modes determined by the excitation frequency. The modes definitely impact the response of the delay line and as can be seen from the Fig. 10, the output response is high for modes other than the SAW modes. Hence, it is desirable to operate the delay line at those bulk and LSAW modes to achieve high electromechanical coupling. Moreover, the impact of the variation of the substrate thickness on the delay line response is described in the following subsection.

5.2. Substrate Thickness Effect

A LSAW propagating along a piezoelectric material with finite thickness is composed of an electric field term and the partial wave components corresponding to the SAW and to the two quasi-shear BAWs. The coupling between these partial waves depends on the properties and orientation of the layer material, the propagation direction as well as on the boundary conditions. When fabricating these devices, the thicknesses of the piezoelectric material layer need to be controlled precisely to obtain the correct delay line operating frequency. The proposed modelling approach is used to demonstrate how the thickness of the piezoelectric substrate is affecting the response of the delay line.

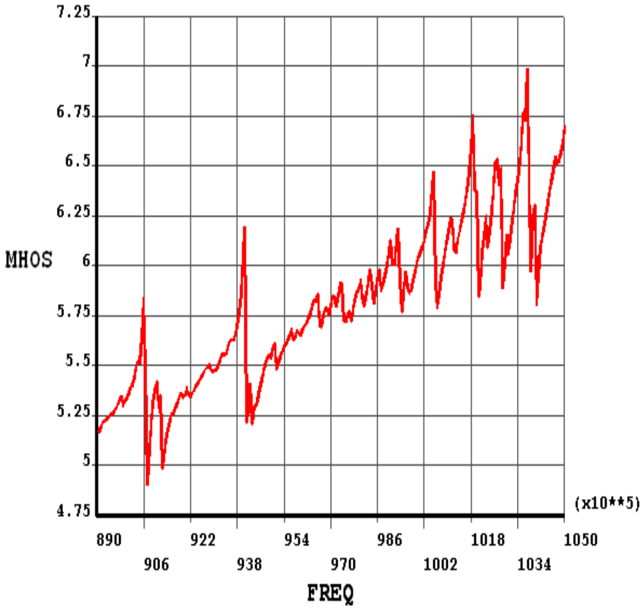

Fig. 9. FEM Admittance magnitude curve.

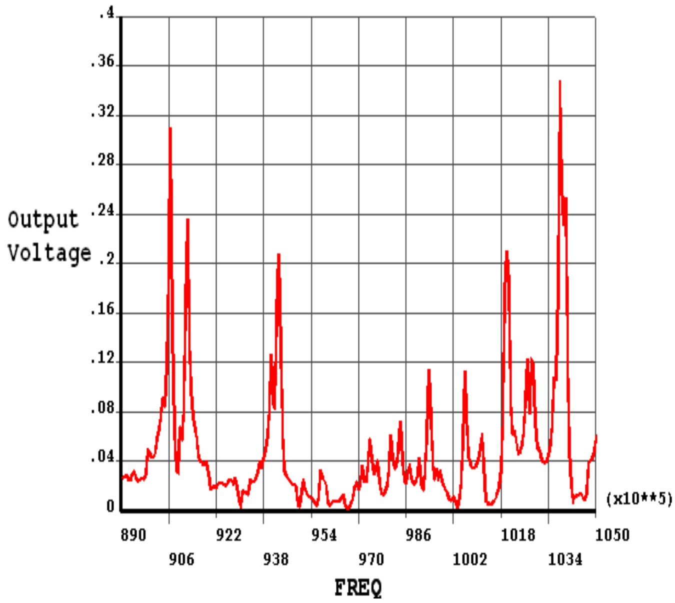

Fig. 10. Magnitude of voltage across the output IDT.

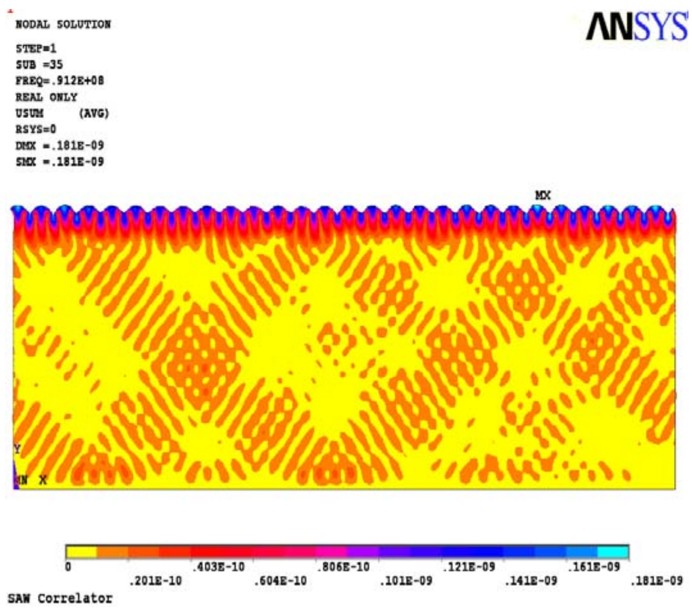

Fig. 11. SAW displacement contour at 91.24 MHz.

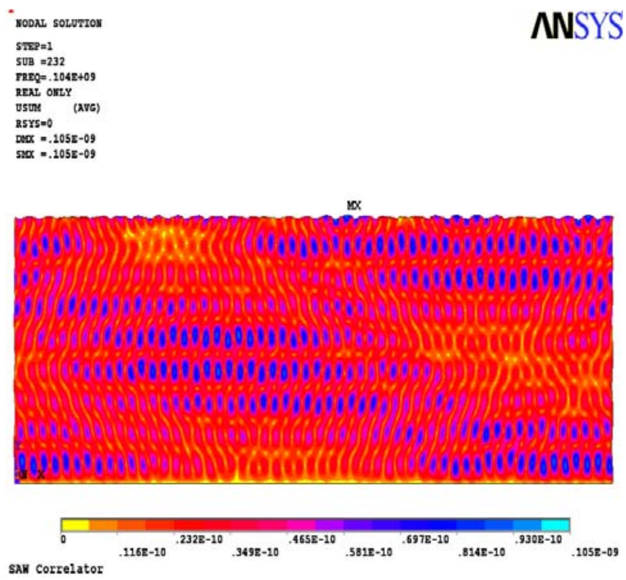

Fig. 12. Leaky SAW displacement contour at 103.84 MHz.

From the above discussed delay line structure, the piezoelectric substrate thickness was reduced to 5λ and harmonic analysis was carried out for a similar frequency range. The electromechanical coupling has improved considerably, as is reflected by the increase in the peak values of the voltage across the output IDT for the LSAW and BAW modes in Fig. 13. As the particle displacement for the SAW modes is mostly confines to the top surface, no considerable changes in the output response was observed with the alteration of substrate thickness.

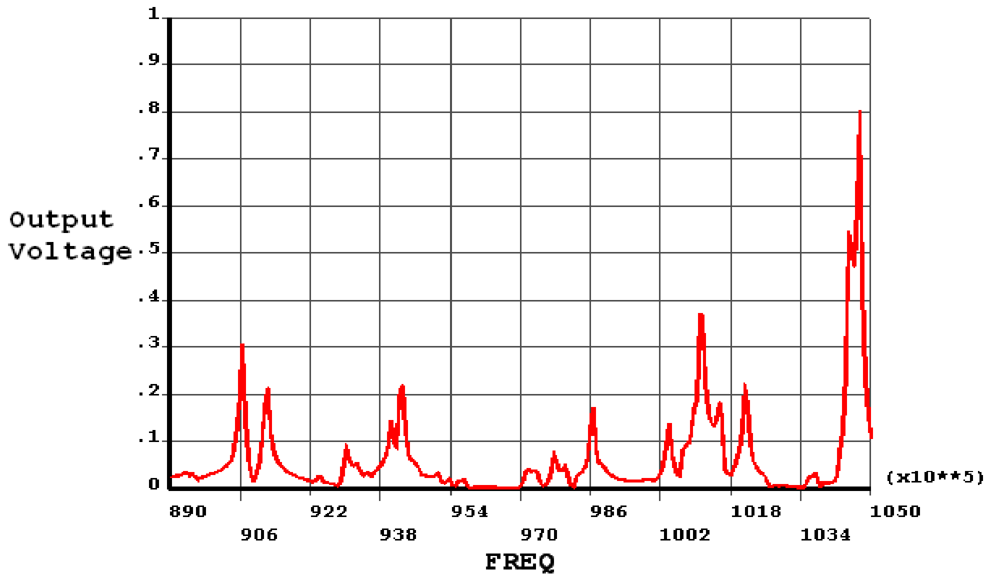

Fig. 13. Magnitude of voltage across the output IDT for a substrate thickness of 5λ.

6. Conclusions

In this paper, finite element modelling approach is used to obtain the eignmodes and the admittance curve for a periodic SAW structure. Then COM/P-matrix parameters are extracted from simulation results using a fitting technique which are in good agreement with measured parameters for similar device specifications, published in the literature. As an example, the practicality of the proposed approach is demonstrated by the modelling of a 2 dimensional delay line with 10 finger pairs per IDT. This allowed the consideration of the complete set of partial differential equations for the calculation of the frequency response of the device for various acoustic modes. The delay line model clearly shows the effect of piezoelectric substrate thickness on the electrical response of the structure. Hence, allowing for device optimisation using different substrate depths.

Acknowledgements

The authors would like to thank the Australian Research Council (ARC) and the School of Electrical and Electronics Engineering (University of Adelaide) for the funding and support for the project.

References

[1]. A. Mamishev, K. Sundara-Rajan, F. Yang, Y. Du and M. Zahn, Interdigital Sensors and Transducers, *Proceedings of the IEEE*, 92, 5, 2004, pp. 808–845.
[2]. I. Jones, L. Ricciardi, L. Hall, H. Hansen, V. Varadan, C. Bertram, S. Maddocks, S. Enderling, D. Saint, S. Al-Sarawi and D. Abbott, Wireless RF communication in biomedical applications, in *Smart Materials and Structures*, Vol. 17, 2008, pp. 015 050: 1–10.
[3]. P. Ventura, J. Hode and M. Solal, A new efficient combined FEM and periodic Green's function formalism for the analysis of periodic SAW structures, in *Proc. of IEEE Ultrasonics Symposium*, 1995, pp. 263–268.
[4]. P. Ventura, J. Hode, M. Solal, J. Desbois and J. Ribbe, Numerical methods for SAW propagation characterization, in *Proc. of IEEE Ultrasonics Symposium*, 1998, pp. 175–186.
[5]. J. Koskela, V. Plessky and M. Salomaa, SAW/LSAW COM parameter extraction from computer experiments with harmonic admittance of a periodic array of electrodes, *IEEE Trans. on Ultrasonics, Ferroelectrics and Frequency Control*, 46, 4, 1999, pp. 806-816.

[6]. K. Hasegawa, K. Inagawa and M. Koshiba, Extraction of all coefficients of coupled-mode equations for natural, single phase by hybrid finite element method, *IEEE Trans. on Ultrasonics, Ferroelectrics and Frequency Control*, 48, 5, 2001, pp. 1341 – 1350.

[7]. M. Hofer, N. Finger, G. Kovacs, J. Schoberl, S. Zaglmayr, U. Langer and R. Lerch, Finite- Element Simulation of Wave Propagation in Periodic Piezoelectric SAW Structures, *IEEE Trans. on Ultrasonics, Ferroelectrics and Frequency Control*, 53, 6, 2006 pp. 1192 – 1201.

[8]. G. Xu, Finite element analysis of second order effects on the frequency response of a SAW device, in *Proc. of IEEE Ultrasonics Symposium*, October 2000, pp. 187-190.

[9]. S. Ippolito, K. Kalantar-Zadeh, D. Powell and W. Wlodarski, A 3-dimensional finite element approach for simulating acoustic wave propagation in layered SAW devices, in *Proc. of IEEE Ultrasonics Symposium*, February 2003, pp. 303-306.

[10]. V. Plessky and J. Koskela, Coupling-of-Modes Analysis of SAW Devices, *International Journal of High Speed Electronics and Systems*, 10, 4, 2000, pp. 867–947.

[11]. C. K. Campbell, Surface Acoustic Wave Devices for Mobile and Wireless Communications, *Academic Press*, Boston, 1998.

[12]. D. Morgan, Cascading formulas for identical transducer P-matrices, *IEEE Trans. on Ultrasonics, Ferroelectrics and Frequency Control*, 43, 5, 1996, pp. 985 - 987.

[13]. M. Hofer, N. Finger, G. Kovacs, J. Scholmer, U. Langer and R. Lerch, Finite Element Simulation of Bulk and Surface Acoustic Wave (SAW) Interaction in SAW Devices, in *Proc. of IEEE Ultrasonics Symposium*, 2002, pp. 53–56.

[14]. Y. Yong, Analysis of periodic structures for BAW and SAW resonators, in *Proc. of IEEE Ultrasonics Symposium*, 2001, pp. 781–790.

[15]. B. Auld, Acoustic Fields and Waves in Solids, ch. Appendix 2, 2nd Edition, *Rober E. Krieger*, 1990.

[16]. A. Tikka, S. Al-Sarawi and D. Abbott, SAW parameter extraction using Finite Element Analysis, in *Proc. of 2nd International Conference on Sensing Technology*, November 2007, pp. 393-398.

[17]. T. Makkonen, V. Plessky, W. Steichen, V. Grigorievski, M. Solal and M. Salomaa, Longitudinal leaky SAW resonators and filters on YZ-LiNbO3, *IEEE Trans. on Ultrasonics, Ferroelectrics and Frequency Control*, Vol. 53, 2006, pp. 393-401.

Guide for Contributors

Aims and Scope

Sensors & Transducers Journal (ISSN 1726-5479) provides an advanced forum for the science and technology of physical, chemical sensors and biosensors. It publishes state-of-the-art reviews, regular research and application specific papers, short notes, letters to Editor and sensors related books reviews as well as academic, practical and commercial information of interest to its readership. Because it is an open access, peer review international journal, papers rapidly published in *Sensors & Transducers Journal* will receive a very high publicity. The journal is published monthly as twelve issues per annual by International Frequency Association (IFSA). In additional, some special sponsored and conference issues published annually.

Topics Covered

Contributions are invited on all aspects of research, development and application of the science and technology of sensors, transducers and sensor instrumentations. Topics include, but are not restricted to:

- Physical, chemical and biosensors;
- Digital, frequency, period, duty-cycle, time interval, PWM, pulse number output sensors and transducers;
- Theory, principles, effects, design, standardization and modeling;
- Smart sensors and systems;
- Sensor instrumentation;
- Virtual instruments;
- Sensors interfaces, buses and networks;
- Signal processing;
- Frequency (period, duty-cycle)-to-digital converters, ADC;
- Technologies and materials;
- Nanosensors;
- Microsystems;
- Applications.

Submission of papers

Articles should be written in English. Authors are invited to submit by e-mail editor@sensorsportal.com 6-14 pages article (including abstract, illustrations (color or grayscale), photos and references) in both: MS Word (doc) and Acrobat (pdf) formats. Detailed preparation instructions, paper example and template of manuscript are available from the journal's webpage: http://www.sensorsportal.com/HTML/DIGEST/Submition.htm Authors must follow the instructions strictly when submitting their manuscripts.

Advertising Information

Advertising orders and enquires may be sent to sales@sensorsportal.com Please download also our media kit: http://www.sensorsportal.com/DOWNLOADS/Media_Kit_2008.pdf